RESEARCH ARTICLE

A New 5G Cellular Broadcasting Approach: Hybrid LDM-NOMA and FeMBMS-OMA Analysis Based on Stochastic Geometry

HEYDAR SHARIATZADEH[1], **SAEED GHAZI MAGHREBI**[1], **BAHATTIN KARAKAYA**[2], **AND ALI SHAHZADI**[3]

[1]Department of Electrical Engineering, Yadegar-e-Imam Khomeini (RAH) Shahre Rey Branch, Islamic Azad University, Tehran 1815163111, Iran
[2]Department of Electrical and Electronics Engineering, Istanbul University-Cerrahpaşa, 34320 Istanbul, Turkey
[3]Department of Electrical and Electronics Engineering, Semnan University, Semnan 3513119111, Iran

Corresponding author: Saeed Ghazi Maghrebi (ghazimaghrebi@jdnasir.ac.ir)

ABSTRACT In this paper, an alternative hybrid infrastructure to complete the media cellular TV puzzle called 5G broadcast is introduced and developed. The performance of a non-orthogonal and orthogonal physical hybrid layer for cellular broadcasting is investigated. A downlink layered division multiplexing with non-orthogonal multiple access (LDM-NOMA) together with a further evolved multimedia broadcast multicast service with orthogonal multiple access (FeMBMS-OMA) is superimposed. In our scenario, we have defined them as two broadcast service providers (BSPs), whereby the former recruits the latter as a cooperative layer. Service selection is done by using a binary factor access technology. We assume that there is perfect knowledge with channel state information for Rayleigh fading multipath channel. Bit error rate (BER) and outage/coverage capacity are selected as our inquiries stochastic geometry benchmarks. The spectrum constellations of the scheme are worked according to the resource block (RB) element/symbols and different modulations. The proposed framework can work without a subscriber identity module (SIM card) uplink and internet protocol (IP). Mathematical analysis, based on the exact closed-form expressions, is consistent with the theory of the proposed LDM-NOMA and FeMBMS-OMA. The simulation results are based on the Monte Carlo iterative methodology, and demonstrate the superiority of the hybrid framework compared to each of the technologies separately.

INDEX TERMS LDM, FeMBMS, 5G broadcast, stochastic geometry (SG), BER, sum rate, outage/coverage probability.

I. INTRODUCTION

Leading innovations within the fifth-generation (5G) broadcasting have been developed since the beginning of the 2020s, and the process still evolving. The exponential growth rate in cellular video broadcast traffic is 30%, and 5G subscriptions are forecasted to reach 5 billion in 2028 [1]. The cellular broadcast coverage through low power low tower (LPLT) stations is growing conventionally and increasing exponentially. Whereas the symmetric trend in 5G broadcasting is towards non-orthogonal and orthogonal convergence cellular broadcast over high power high tower (HPHT) stations

The associate editor coordinating the review of this manuscript and approving it for publication was Oussama Habachi.

[2], [3], [4]. Therefore, the number of service providers (SPs), which each covers its own set of users will be increased. There are infrastructure radio gaps among SPs for cellular broadcast multi-region LPLT and HPHT coverage, according to cellular technology, and diverse radio access technologies (RATs). Moreover, the SPs have promoted standard-definition television (SDTV) to high-definition television (HDTV), and hence, the quality of service is increased with complete coverage of the borders and edges. The combination technology offers several opportunities and challenges regarding future cellular broadcast recipients as well as 5G broadcast service [5], [6], [7]. A historical analysis of cellular broadband generations demonstrates that it is modified nearly once a decade, while television broadcast technology changes over time [8].

Today, SPs owners are seeking another option for the next cellular broadcast via a current hybrid platform layer technology, which can be an alternative to cellular broadcasting and is compatible with existing service providers. Furthermore, the international telecommunication union (ITU) and the radio frequency regulations organization have imposed restrictions. These restrictions have reduced broadcast bandwidth and increased cellular broadband, which is called digital dividend [9]. Incompatibility and contradiction in digital terrestrial television broadcasting (DTTB) infrastructure have been a historical challenge in cellular broadcast technology for BSP and mobile recipients. There was incompatibility in the 3G technology era for wide band code division multiple access against digital video broadcasting handheld in broadband and broadcast, respectively [10], [11].

Lately, broadcast owners and network developers have suggested a juxtaposition approach to address these challenges. In the last few years, researchers considered it a likely solution to implement hybrid technology via a multi-layer delivery system. The hybrid broadcast technology family can provide soft guarantees on network switching performance. The NOMA-based family has been recently combined with various multiple-access conventional OMA-based techniques. The hybrid framework is proposed as a middle technology between mobile broadband and stationary broadcast [12], [13], [14].

The convergence of orthogonal, e.g., digital terrestrial video broadcasting (DVB-T2) and non-orthogonal, e.g., 5G, in content and technology is one of the developments of the last decade in the field of media. This approach is called hybrid-cast in Japan and Ginga in Brazil. In the formation of the convergence of broadcast and broadband in all layers, especially the physical layer, a new platform is created that can cover HPHT and LPLT users [15], [16].

In particular, hybrid systems offer more freedom By exploiting different areas such as power, frequency, and domain code to serve many users. Therefore, hybrid systems are able to achieve the widespread connectivity expected in the 5G and 6G broadcast generations of dense wireless networks. Whereby, the available spectrum for transmission is divided into several sub-bands, i.e., channels, where multiple users are served simultaneously in each sub-band with the NOMA power range [17], [18], [19].

The 3rd Generation Partnership Project (3GPP) introduced evolved Multimedia Broadcast Multicast Services (eMBMS) for 4G long-term evolution (LTE) in Rel-9 as a point-to-multipoint communication, which is known as LTE-broadcast (LTE-B) as an orthogonal service provider. The LTE-B naturally fits with trends for mobile video content demand, which in the short term will make up at least 70% of all data traffic [20], [21]. Newly, the 3GPP enhancements for broadcast have offered a further evolved MBMS (FeMBMS). It is a remarkable development of the LTE broadcast mode eMBMS in 3GPP. Also, Rel-14, Rel-16, and Rel-17 versions identify called as 5G broadcast, and this is founded based on

4G LTE. Formerly, up to 60% and 40% of sub-frames have been allocated in the eMBMS Rel-13, to broadcast and unicast modes, respectively. Nowadays,the feature has become flexible in capacity to improve broadcast participation, which can appropriate up to 100% sub-frames to enable transmission capacity to be used for broadcasting services and as a result allows larger transmitter cells in a single frequency network [22], [23], [24].

Moreover, multi-carrier layered division multiplexing (MC-LDM), denoted as LDM, by dedicating different power worthiness to each user, is a sub-section of power division-non orthogonal multiple access (PD-NOMA) which is a form of physical-layer non-orthogonal uses and available spectrum resource block (RB) The foundation of LDM technology is based on two layers to wit, the top layer, and the bottom layer. We use the LDM standard to provide maximum ruggedness against multi-path interference downlink in the case of the Rayleigh fading channel [25], [26]. Unlike previous studies, we demonstrate a hybrid of LDM and FeMBMS frameworks for cellular broadcast transmission, from a technological selection perspective.

To clarify the performance of our proposed design, mathematical analysis and simulation are employed through relationships formulated systems individually for LDM and FeMBMS. The BER and outage probability are derived and simulated for each broadcast service provider and hybrid technology. The power is allocated through the application of the fractional transmit power allocation (FTPA) algorithm for LDM RB sub-carriers with the ξ decay factor [27]. Moreover, BER and outage probability mathematical analysis are derived based on the number of sub-carriers per RBs in the spectrum [28].

Proposition: Suppose a base station (BS) is working in a single-cell network with two different mobile TV broadcast service providers (BSPs). Each operator has its own local user as U is denoted. For example, traditional OMA has a subset of total users and current NOMA has a sub-set of total users. Each NOMA has m RBs and two users per subcarrier, while OMA has m' RBs and a user per sub-carrier. Therefore, each BSP produces a different instantaneous throughput at a given time. Accordingly, a BSP operator has a minimum rate required for the activity of its users in the cell, which is also defined as the probability of outage or interruption [29]. In our scenario, FeMBMS-OMA is first and LDM-NOMA is second BSPs.

Illustration: Figure 1 illustrates a simplified proposed framework containing a next-generation base station (gNB) with a single cell. In this figure, a single input single output (SISO) antenna downlink is transmitted broadcasting. The BSP1 and BSP2 superimpose and broadcast orthogonal FeMBMS signal and non-orthogonal LDM signal, in a single-tier cellular network, respectively. LDM-LL is a fixed broadcast service with a high rate of data, and LDM-UL is a mobile broadcast service. BSP1 and BSP2 are working with two orthogonal/non-orthogonal radio frequencies. D_{UL}, D_{LL},

D_{FeMBMS} denotes the distance from the LDM far user (FU), near user (NU), and FeMBMS user in the gNB, respectively. The LDM and FeMBMS simultaneously transport two users per sub-carrier and one user per sub-carrier in a channel, respectively. The user with a strong received signal to transport fixed services, is the lower layer (LL) which has a less transmission power, a superior-level modulation, and a greater signal constellation to transport fixed services. The upper layer (UL) is the farthest user with a weak received signal equipped with a low-level modulation, superior transmission power, and a smaller signal constellation that carries mobile services. The FeMBMS is an variable user with a superior-level modulation, low transmission power, and a greater signal constellation which carries mobile and fixed services [5], [30]. In addition, the closest user with a higher channel quality factor is called h_{LL}, and the farthest user with a lower channel condition factor is called h_{UL} from the gNB. For instance, the UL, LL, and FeMBMS are applied to a binary phase-shift keying (BPSK), a quadrature phase-shift keying (QPSK),and a QPSK modulation, respectively.

A. RELATED WORKS

Rohde & Schwarz in [2] demonstrated the latest 5G Broadcast enabling technology in Mobile World Congress (MWC) 2023 Barcelona, Spain, and exhibited using an HPHT network topology as an overlay for mobile networks, the transmission will be significantly more efficient and cost-effective than before. The authors in [6] and [14] are expressed that the hybrid NOMA/OMA family can offer a suitable combination for 5G Broadcast. Zhang et al. [17] expressed that there are practical approaches to realizing capacity in power-based-NOMA systems. The use of a hybrid TDM-LDM structure is suggested to increase capacity gains. Ghosh et al. [31] compared NOMA technology with OMA for mmWave massive multi input multi output (MIMO). Sharnil et al. [19] analyzed a hybrid NOMA-OFDM 5G multiuser wireless system using a deep neural network. Baghani *et al.* [29] introduced a selection technology between NOMA and OMA that is dynamically based on the instantaneous downlink channel. The authors in [32] and [33] studied the problem of analytically the closed-form BER expressions for non-orthogonal with two and three users using BPSK and QPSK modulation schemes. The authors in [34], [35], and [36] expanded about the Hybrid NOMA/OFDMA with different approaches. Tusha et al. [37] illustrated a hybrid power domain employing an orthogonal/non-orthogonal framework for downlink transmission with two UDs. Shokair et al. [38] argued that a hybrid broadcast/broadband network is a potential solution to mitigate the increasing demand for mobile TV. According to the channel condition. Al-Abbasi and So [39] proposed the hybrid schemes technology, which is outperformed the separate method due to its flexibility in adapting the transmission approach. Bariah et al. in [40] has investigated the error rate of LDM system performance over Nakagami-*m* and Rayleigh fading channels. The idea of using a combination

of OFDMA and PD-NOM in cellular broadcast network has been studied over years by Marcano et al. [41] and Zhang et al. [42] characterized the mobile service delivery capability of the LDM-NOM system with various challenging wireless propagation environments, considering both analysis and extensive simulations. Gimenez et al. [24] proposed a joint NR-MBMS which includes FeMBMS broadcasting.

ETSI TR 126 report in [43] announced digital television terrestrial broadcasting (DTTB) services, which will be delivered over the eMBMS system. Zhang et al. [44] presented a non-orthogonal MBMS transmission scheme in a K-tier single-frequency heterogeneous network and also they studied two main usage scenarios: Multi-rate and multi-service MBMS transmission. Assaf et al. [45] derived and developed the exact and closed-form BER expressions using arbitrary square M-QAM per user without modulation constraint orders for non-orthogonal technology. Maksymyuk et al. [46] introduced basic stochastic geometry models which provides good understanding of the mobile network behavior. Table 1 gives the last five years study on comparative hybrid orthogonal/non-orthogonal related work that highlights different technologies with proposal schemes. Whereby,in this research, we investigate a cellular hybrid broadcast and broadband non-orthogonal/orthogonal LDM/FeMBMS framework to rectify the aforesaid bugs occasions. Based on the earlier discussions, also we study the cellular system from a technological viewpoint. The contributions of this work are manifold as follows

B. CONTRIBUTIONS AND ORGANIZATION

- We are looking for an alternative to have a physical layer to complete the broadcast media puzzle for 5G cellular broadcasting.
- From the user service point of view, there are ways to increase 5G capacity gains. One of these methods is the non-orthogonal/orthogonal hybrid approach proposal.
- From the point of convergence view we look at the issue of hybrid broadcast and broadband.
- In terms of technology selection, a hybrid novelty in cellular 5G broadcast HPHT technology is introduced, in which the BSPs are selected by RAT in hybrid form or individually.
- We offer a method for intermediate multi-rate/multi-service selection by using two BSPs as a hybrid of non-orthogonal LDM-NOMA and orthogonal FeMBMS-OMA broadcasting technologies.
- The two BSPs are used to complete cellular coverage regions in the transition between broadcast/broadband generations of the border for edges. For example 4.5G and 5G.
- The proposed system is able to work in conditions without a shared identity module (SIM card) for uplink and Internet Protocol (IP) due to broadcast technology attributes.

The rest of the article is organized as follows. In section II, a stochastic geometry perspective is introduced. In section III,
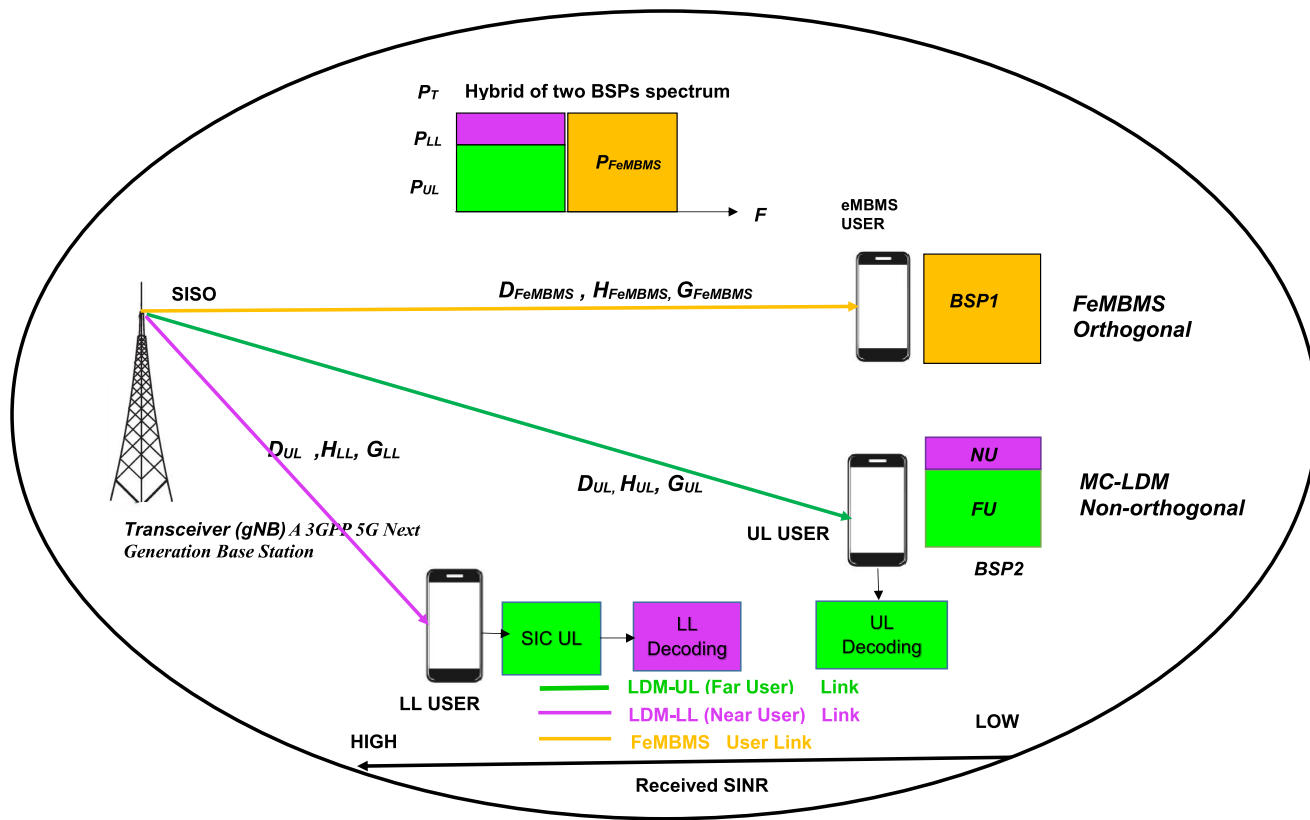
FIGURE 1. Illustrative diagram of the three-layers cellular broadcast proposed system model.

the system model description is given. In section IV, Performance analysis in sub-sections (modulation schemes/ rate and outage/coverage) is investigated. In section V, the FTPA for LDM is presented. In section VI, the simulation results are given in sub-sections (BER, FTPA, outage/coverage) are brought. In VII, the conclusions and future ideas are given.

II. A STOCHASTIC GEOMETRY PERSPECTIVE
The BSPs usually are modeled by the locality of the base stations according to a traditional geometry such as a hexagonal grid and are modeled by the BS location with mobile users either randomly scattered or placed deterministically. Typically, Wyner's model has been widely used to model and analyze cellular networks due to its simplicity and analytical tractability [47]. Traditional models such as hexagonal are unrealistic, but with the expansion of multi-tier cellular networks, the reality of network geometry has changed and previous models are not able to analyze network behaviors. We will analyze and simulate two criteria performances based on stochastic geometry, outage, and coverage probability. The outage probability is a criterion for the probability density function, which is a derivative of the cumulative distribution function of signal-to-interference plus noise ratio (SINR). Also, it is the complement of coverage probability. These functions in a stochastic approach are provided by a realistic description of the cellular network compared to a grid

model. The gNB is located at the center of a hexagonal geometry cell, which is equipped with SISO antennas. The Poisson point process (PPP) is a simple process that is easily tractable to model heterogeneous networks with infinite number of nodes in an unlimited coverage area. Also the hard core point process model is the most suitable to design small cell coverage within one tier of the heterogeneous network providing the most accurate distances between co-channel transmitters [48], [49]. To this end, PPP is used to model the positions of the users in the proposed hybrid LDM/FeMBMS technology and expanded outage/coverage probability in subsection IV-B.

III. SYSTEM MODEL DESCRIPTIONS
In this section, the proposed hybrid framework is described, and then followed by the main mathematical derivations are given. The annotations symbol definitions associated with joint LDM/FeMBMS technologies are summarized in Table 2. The block diagram transceiver is introduced and equipped as variable M resource block that includes variable K sub-carriers and U users. Moreover, there are two types of RBs, the LDM denotes ψ, and the FeMBMS resource blocks denote Ω and each group includes several sub-carriers. The user device (UD) and BS are equipped with SISO antennas. Moreover, the FeMBMS orthogonal signal is superimposed on the same frequency and time slot architecture. In the

TABLE 1. Related study hybrid orthogonal/non-orthogonal that highlights different technologies with the proposed scheme in the last five years.

References	Algorithm Description	Different Technology	Evaluation Criteria	Type of Network
[25], **2017**	Mobile TV	Hybrid LTE-4G/eMBMS-LDM	LDM-eMBMS Capacity / sum rate	Multi-user
[39], **2017**	Optimization/User paring	Hybrid Multiple Access OMA/NOMA	Coverage probability, sum rate	Two-user
[29], **2018**	Optimization using DC programming	Hybrid NOMA/OMA in 5G Dynamicly	Achivable utility/sum rate, Outage probability	Two users
[24], **2019**	New Radio Approach	Hybrid Broadcast/Multicast FeMBMS	SINR, LPLT/HPHT for NR-MBMS	MFN/SFN
[38], **2019**	Stochastic Geometry	Broadcast/Broadband Hybrid	Probability Coverage, Spectral efficiency, Power efficiency	Two users
[26], **2019**	Using Multiplexing to Deliver Mobile TV	Hybrid DTV LDM Multi-Layer	LDM-CL fixed, LDM-EL mobile Receivers performance	Multi-user
[36], **2020**	Deep Reinforcement Learning	Hybrid NOMA/OMA 5G Networks	Average Rate, EE, PA	Multi-user
[31], **2021**	MIMO investigation	Hybrid H-NOMA	SE, EE and Outage probability	Multi-user
[35], **2021**	Using DFT-S-OFDM	Hybrid Orthogonal/Non-orthogonal	Fairness-aware, BER, Rate	Multi-user
[37], **2022**	Indexed Modulation IM-NOMA/OFDM-IM	Hybrid NOMA/OFDM index modulation	BER, sum rate	Two-users
[34], **2022**	Two-dimensional Power Allocation/VLC system	Hybrid NOMA/OFDMA	Symbol Error Rate, BER	Multi-user
[19], **2022**	Deep Neural Network Branch-and-bound algorithm	Analysis Joint NOMA-OFDM 5G wireless	BER, various SNR, Optimization	Multi- user
[14], **2022**	Technical Specification	Hybrid 5G Multicast-Broadcast	FeMBMS Architectural enhancements	Release 17
[2], **2023**	5G broadcast Approach	Hybrid 5G Broadcast	Mobile World Congress (MWC)	Multi-user
This work	5G broadcast Approach	Hybrid LDM-NOMA and FeMBMS-OMA	sum rate, BER, Outage/Coverage	Multi-user

transmitter part of the system model, as shown in Figure 2 (a), the transport RBs data is produced in two-original ways, FeMBMS and LDM. The LDM-UL and LL data pass the gray coding and are sent to the bit-interleaved coding and modulation (BICM) processing chain. In the BICM, bits after rate matching is concatenated, scrambled, and mapped to constellation symbols. The available modulation schemes for LDM-NOMA and FeMBMS-OMA are BPSK, and QPSK, respectively. Then a program stream (PS) in a multiplex is generated and a transport stream (TS) is made from PSs in re-multiplex [50]. After that, the TSs are allocated to all the available RB in the corresponding sub-carrier, and finally the cyclic prefix will be inserted. The TS content through the orthogonal frequency division multiplexing (OFDM) chain will be converted from the time domain to the frequency domain on the RF channel. As shown in equation (1), the result is multiplied by the g factor and injection power level factor, and then the two layers are superposed together

in the power domain. By utilizing the g factor, related to power adjustment at the transmitter, the LDM-UL and LL powers are normalized to one. This means that the total power of each layer equals one. The FeMBMS-OMA signal after passing the gray coding is multiplexed with the LDM part. The hybrid LDM/FeMBMS deterministic signal is transformed from serial to parallel. After that, the hybrid LDM/FeMBMS signal is modulated. Then it generates a total transmitting signal. As shown in Figure 2 (b), the receiver blocks work inverse exactly to the transmitter blocks chain. Figure 3, illustrates frequency spectrum RBs for LDM as ψ and FeMBMS as Ω versus the power domain separately. The PLL and PUL are two LDM power levels and P_{FeMBMS} are single FeMBMS power levels, in which BS total power level is the equal summation of $P_{LL} + P_{UL} + P_{FeMBMS} = 1$, the total system bandwidth is fixed (for e.g, 5 MHz) in our simulation, and the two technologies are adjacent to each other.
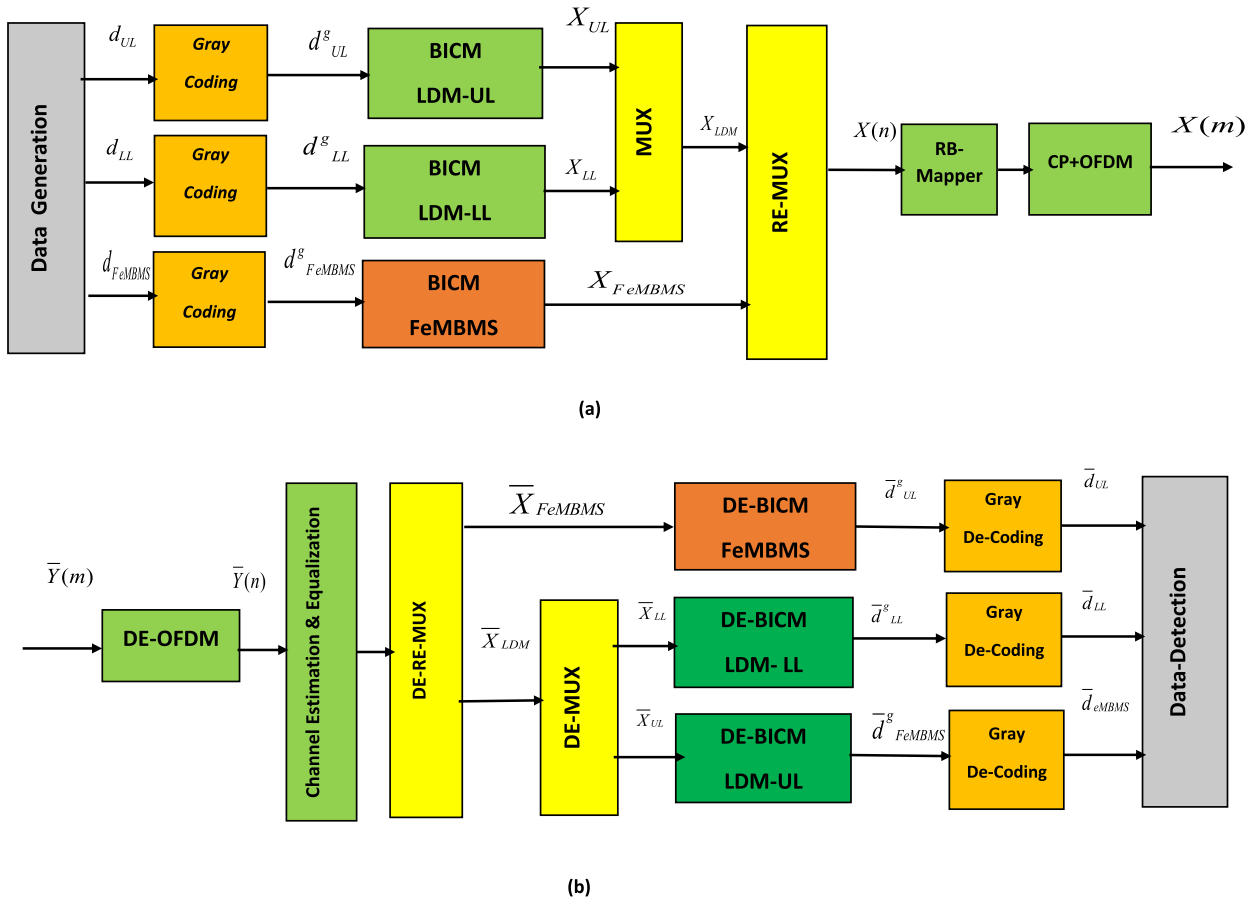
(a)

(b)

FIGURE 2. Block diagrams of the Non-orthogonal/Orthogonal hybrid LDM-NOMA/FeMBMS-OMA (a) TX (b) RX.
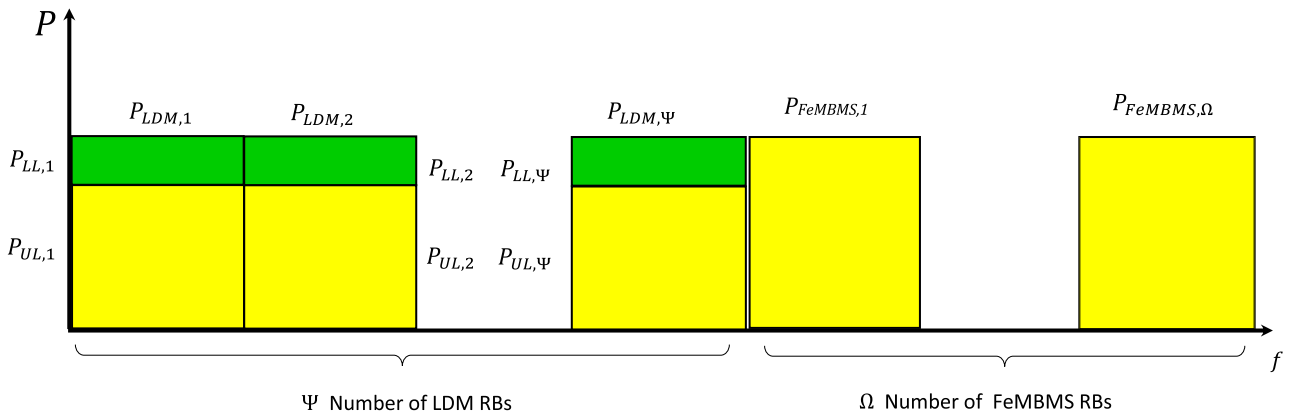

FIGURE 3. Layout of the Non-orthogonal/Orthogonal hybrid LDM-NOMA/FeMBMS-OMA frequency spectrum of RBs.

A. SYSTEM BASIC FORMULATION

A combination of transmitted frequency signals for LDM and FeMBMS with M RBS and K sub-carriers is given as below.

$$X_m[k] = \alpha_m X_{LDM,m}[k] + \beta_m \sqrt{p_{FeMBMS}} X_{Fe.,m}[k]$$
$$\text{for } m = 1, 2, \ldots, M \text{ and } k = 1, 2 \ldots, K_m \quad (1)$$

where α_m and β_m are dedicating indexes to mth RB for LDM and FeMBMS systems respectively. To select the mth RB from LDM symbols we assign binary factor $\alpha_m = 1$ and $\beta_m = 0$, and to select the RB from FeMBMS symbols, we assign binary factor as $\beta_m = 1$ and $\alpha_m = 0$. The $X_{LDM,m}[k]$, is the token transported in the kth sub-carrier of mth RB in LDM section, that is equal to summation of UL

TABLE 2. Symbol definitions.

Parameter	Definition
P_T	Total transmission power from the gNB site
P_{LDM}	Total power of LDM technology
P_{UL}	Total power of LDM upper layer
P_{LL}	Total power of LDM lower layer
P_{FeMBMS}	Total power of FeMBMS technology
ps	Per Subcarrier
g	Injection power factor
B	Total Bandwidth
RB	Resource Block
U	Total number of Users
M	Total number of resource blocks
Ψ	Total number of LDM resource blocks
Ω	Total number of FeMBMS resource blocks
γ	Signal to Noise Ratio (SNR)
K	Total number of sub-carriers
m	Resource block index
S	A subset of broadcast service providers
n	Time-domain sample index
k	Frequency domain index
K_{LDM}	Total number of LDM sub-carriers
K_{FeMBMS}	Total number of FeMBMS sub-carriers
N	Fast Fourier Transform (FFT) points
T	Useful time duration of multi-carrier symbol
α_m	The binary index for mth RB illustrates where LDM is allocated
β_m	The binary index for mth RB illustrates where FeMBMS is allocated
$N0$	Additive White Gaussian Noise
Pr_{out}	The outage probability based on capacity
$\bar{\gamma}_{FeMBMS}$	The FeMBMS average SNR
C_{PTP}	Total point-to-point channel capacity
$P_{Hybrid}(e)$	Total hybrid power error probability
$G_{UL}[k]$	The LDM UL frequency channel gain
$G_{LL}[k]$	The LDM LL frequency channel gain
$G_{FeMBMS}[k]$	The FeMBMS frequency channel gain
$x(t)$	Time-domain transmit signal
$y(t)$	Time-domain received signal
$x(n)$	The discrete transmit signal
X_{LDM}	The LDM transmit signal
X_{FeMBMS}	The FeMBMS transmit signal
$X_m[k]$	The discrete transmission signal in the frequency domain
$\mathbf{Y}$	The total vector of the received discrete signal after the FFT block in the frequency domain
$Y_m[k]$	The discrete signal recipient at kth sub-carrier, which belongs to mth RB
$y(n)$	Overall discrete signal recipient
$H[k]$	The base-band discrete channel frequency response
$\hat{X}_m[k]$	Estimated and equalized signal transmitted in the mth RB
$\bar{P}_{UL}(e)$	Average error probability of LDM UL
$\bar{P}_{LL}(e)$	Average error probability of LDM LL
$H_{LL}[k]$	Channel frequency response of the LL at kth sub-carrier
$H_{UL}[k]$	Channel frequency response of the UL at kth sub-carrier
$H_{FeMBMS}[k]$	Channel frequency response of the FeMBMS at kth sub-carrier
$\bar{P}_{LDM}(e)$	The average error probability of the LDM
$\bar{P}_{FeMBMS}(e)$	The average error probability of the FeMBMS
R_{FeMBMS}	The FeMBMS sum rate
R_{LDM}	The LDM sum rate
R_T	Total sum rate
d_{UL}^g	Data after UL gray coding
d_{LL}^g	Data after LL gray coding
d_{FeMBMS}^g	Data after FeMBMS gray coding
d_{LL}	Data before gray coding

symbol $X_{UL,m}[k]$ and LL symbol $X_{LL,m}[k]$. The $P_{UL,m}[k]$ and $P_{LL,m}[k]$ notations are called LDM transmitted powers. Therefore, the beamforming BSP powers for a transmission over mth RBs will be determined by

$$X_{LDM,m}[k] = \sqrt{P_{UL}}X_{UL,m}[k] + \sqrt{P_{LL}}X_{LL,m}[k]. \quad (2)$$

$$X_m[k] = \alpha_m \left(\sqrt{P_{UL}}X_{UL,m}[k] + \sqrt{P_{LL}}X_{LL,m}[k] \right) + \beta_m X_{FeMBMS}[k]. \quad (3)$$

$$\text{for } m = 1, 2, \ldots, M \text{ and } k = 1, 2, \ldots, K_m$$

Accordingly in an LDM RB, there can be two group users and for FeMBMS RB, only the first group user will be assigned. The LL sub-carrier power is changed by the injection level of g and the summation, power is normalized to P_{LDM}. Hence, the transmit powers of LL and UL can be written in terms of P_{LDM} as follows

$$P_{LL} = \frac{g}{1+g}P_{LDM} \text{ and } P_{UL} = \frac{1}{1+g}P_{LDM}. \quad (4)$$

We assume equal power allocation to the RBs. Hence, the power of the LDM part can be computed by

$$P_{LDM} = P_T \frac{\Psi}{M} \quad (5)$$

$Y_m[k]$ is called user signal and is decoded from LDM or FeMBMS sub-carrier its own RBs are introduced as follows

$$Y_m[k] = X_m[k]H_m[k] + W_m[k]$$
$$\forall m \in \{1, 2, \ldots, M\}. \quad (6)$$

In our framework, we assume perfect channel condition information, the channel is frequency-selective and time-varying for broadband mobile multi-path broadcasting. We use channel estimation and equalization. The linear estimation for an arbitrary signal from another interference signal, channel estimation can also be done using the frequency domain approach. It decreases mainly the computational complexity in the time domain. Channel equalization is the process of reducing amplitude, frequency, and phase distortion in a channel in order to improve transmission performance. Channel equalization is carried out after channel estimation. We put in Figure 2 (b) the channel estimation and equalization block in receiver. Hence, the estimated transmit signal at mth RB can be found as below

$$\hat{X}_m[k] = \frac{Y_m[k]}{H_m[k]}. \quad (7)$$

If the frequency spectrum of the RBs access are selected on the FeMBMS user ($\alpha_m = 0$), detection of the user data, $\hat{d}_{FeMBMS,m}$, will be done with the estimated signal. However, if the RB is used for the LDM signal the UL user data detection, $\hat{d}_{UL,m}$, will be done after the signal de-normalized. The $\hat{d}_{LL,m}$ is LL user data detection, successive interference cancellation (SIC) procedure is followed by using LL receiver [51]. This is done due to the LL user being the nearest user to the gNB station compared to the UL user and the LL user can

remove the inter-user interference from the UL user which convinces the SIC states $G_{LL}[k] > G_{UL}[k]$. Where $G_{LL}[k]$ and $G_{UL}[k]$ are the channel gains and are determined as follows

$$G_{LL}[k] = \frac{|H_{LL}[k]|^2}{N_{0,LL}} \quad (8)$$

$$G_{UL}[k] = \frac{|H_{UL}[k]|^2}{N_{0,UL}} \quad (9)$$

IV. PERFORMANCE ANALYSIS

A. BER EVALUATION VERSUS MODULATION SCHEMES

In this sub-section, we evaluate the performance of the considered system for three different modulation schemes, i.e., BPSK-BPSK/QPSK and QPSK-BPSK/QPSK and QPSK-QPSK/QPSK for LL and UL, FeMBMS users respectively.

1) BPSK-BPSK/QPSK

The BPSK-BPSK/QPSK modulation schemes introduce closed-form equations. The average BER performance for a single carrier and a closed-form expression of NOMA uplink/downlink for FU and NU with different modulations are derived in [32] and [33]. Since their work was a single carrier system for a flat fading channel, some hand-works are demanded to catch rules in accordance with the multi-carrier system and multi-path Rayleigh channel assumption in the case of frequency selective small scale [52]. The error probability of the UL is as below

$$\overline{P}_{UL}(e) = \frac{1}{4}\left[\left(1 - \sqrt{\frac{\bar{\gamma}_A}{2+\bar{\gamma}_A}}\right) + \left(1 - \sqrt{\frac{\bar{\gamma}_B}{2+\bar{\gamma}_B}}\right)\right] \quad (10)$$

where

$$\bar{\gamma}_A = \frac{(\sqrt{2P_{UL}} + \sqrt{P_{LL}})^2 E\{|H_{UL}|^2\}}{N_0} \quad (11)$$

and

$$\bar{\gamma}_B = \frac{(\sqrt{2P_{UL}} - \sqrt{P_{LL}})^2 E\{|H_{UL}|^2\}}{N_0} \quad (12)$$

Here, $E\{.\}$ is the expectation operator. The notations $\bar{\gamma}_A$ and $\bar{\gamma}_B$ are the average signal-to-noise ratios (SNRs) for the different signal constellation points for superimposed BPSK modulated UL symbols and QPSK modulated LL symbols, respectively. The error probability of the lower layer (LL) is as below

$$\overline{P}_{LL}(e) = \frac{1}{2}\left(1 - \sqrt{\frac{\bar{\gamma}_C}{2+\bar{\gamma}_C}}\right)$$
$$+ \frac{1}{8}\left[\sqrt{\frac{\bar{\gamma}_D}{2+\bar{\gamma}_D}} - \sqrt{\frac{\bar{\gamma}_E}{2+\bar{\gamma}_E}}\right.$$
$$\left. - \sqrt{\frac{\bar{\gamma}_F}{2+\bar{\gamma}_F}} + \sqrt{\frac{\bar{\gamma}_G}{2+\bar{\gamma}_G}}\right] \quad (13)$$

where

$$\bar{\gamma}_C = \frac{P_{LL}E\{|H_{LL}|^2\}}{N_0} \quad (14)$$

$$\bar{\gamma}_D = \frac{(\sqrt{2P_{UL}} + \sqrt{P_{LL}})^2 E\{|H_{LL}|^2\}}{N_0} \quad (15)$$

$$\bar{\gamma}_E = \frac{(\sqrt{2P_{UL}} - \sqrt{P_{LL}})^2 E\{|H_{LL}|^2\}}{N_0} \quad (16)$$

$$\bar{\gamma}_F = \frac{(2\sqrt{2P_{UL}} + \sqrt{P_{LL}})^2 E\{|H_{LL}|^2\}}{N_0} \quad (17)$$

$$\bar{\gamma}_G = \frac{(2\sqrt{2P_{UL}} - \sqrt{P_{LL}})^2 E\{|H_{LL}|^2\}}{N_0} \quad (18)$$

where, the equations (14)–(18) are definitions of average SNRs. The error probability in [53] and also localized in the FeMBMS part can be written as follows

$$\overline{P}_{FeMBMS}(e) = \frac{1}{2}\left(1 - \sqrt{\frac{\bar{\gamma}_{FeMBMS}}{2+\bar{\gamma}_{FeMBMS}}}\right) \quad (19)$$

We define a criterion for the channel gain response normalized by noise (CRNN) and it is denoted as $G_{m,n} = \frac{|h_{m,n}|^2}{\delta_k^2}$ [54]. Where $h_{m,n}$ is the channel coefficient of RBm from the gNB to UEs and δ_k^2 is the noise variance of kth sub-carrier in RBs and then we localize it in sub-section (IV-A). Where in equation (19), $\bar{\gamma}_{FeMBMS}$ is the average SNR of the QPSK modulated FeMBMS symbols and is introduced as follows

$$\bar{\gamma}_{FeMBMS} = \frac{2P_{FeMBMS}E\{|H_{FeMBMS}|^2\}}{N_0} \quad (20)$$

and $\bar{G}_{FeMBMS}$ is the average channel gain response of the QPSK modulated FeMBMS as below

$$\bar{G}_{FeMBMS} = \frac{E\{|H_{FeMBMS}|^2\}}{N_{0,FeMBMS}}. \quad (21)$$

To recognize the efficacy of the number of RBs on the LDM or FeMBMS part, we describe the average total BER of the proposed hybrid system is as follows

$$\overline{P}(e) = \frac{\Psi(k_{LL} + k_{UL})\overline{P}_{LDM}(e) + \Omega k_{FeMBMS}\overline{P}_{FeMBMS}(e)}{\Psi(k_{LL} + k_{UL}) + \Omega k_{FeMBMS}} \quad (22)$$

where $k_{LL} = \log_2 M_{LL}$ and $k_{UL} = \log_2 M_{UL}$ denotes the number of bits per LL and UL symbols, respectively. Here M_{LL} and M_{UL} denotes the order of LL and UL symbol modulations. $\overline{P}_{LDM}(e)$ denotes the average BER of the LDM part and can be written as

$$\overline{P}_{LDM}(e) = \frac{1}{k_{LL} + k_{UL}}\left(k_{LL}\overline{P}_{LL}(e) + k_{UL}\overline{P}_{UL}(e)\right) \quad (23)$$

2) QPSK-BPSK/QPSK

In the QPSK-BPSK/QPSK three services modulation orders case, we suggested average BER performance closed-form expression for downlink multi-carrier hybrid framework for three users. We update [24, [45]] to suit our proposed system as follows

$$\overline{P}_{UL}(e) = \frac{1}{8} \sum_{i=1}^{6} V_i \left(\sqrt{\frac{\bar{\gamma}_i}{2 + \bar{\gamma}_i}} \right) \qquad (24)$$

where $V_i = [3, 3, 2, 2, 2, 2]$ is index vector.

$$\overline{P}_{LL}(e) = \frac{1}{4} \left[\sum_{i=5}^{12} V_{i,a} \left(\sqrt{\frac{\bar{\gamma}_i}{1 + \bar{\gamma}_i}} \right) - \sum_{i=13}^{18} V_{i,b} \left(\sqrt{\frac{\bar{\gamma}_i}{1 + 2\bar{\gamma}_i}} \right) \right] \qquad (25)$$

where $V_{i,a} = [4, -3, 3, 2, 2, -1, 1]$ and $V_{i,b} = [3, -3, 2, -2, 1, -1]$ are index vectors.

$$\overline{P}_{Hybrid}(e) = \overline{P}_{UL}(e) + \overline{P}_{LL}(e) + \overline{P}_{FeMBMS}(e) \qquad (26)$$

3) QPSK-QPSK/QPSK

In special QPSK-QPSK/QPSK modulation schemes, we offered average BER performance closed-form expression for downlink multi-carrier LDM/FeMBMS framework for three users. Also, now using the equation (26) for the hybrid proposed system and update [27, [45]] to suit our proposed system as follows

$$\overline{P}_{UL}(e) = \frac{1}{4} \sum_{i=1}^{2} \frac{1}{2} \left(1 - \sqrt{\frac{\bar{\gamma}_{ul,i}}{2 + \bar{\gamma}_{ul,i}}} \right) \qquad (27)$$

$$\overline{P}_{LL}(e) = \frac{1}{2} \sum_{i=1}^{5} V_{ll,i} \left(\sqrt{\frac{\bar{\gamma}_{ll,i}}{1 + \bar{\gamma}_{ll,i}}} - \sqrt{\frac{8\bar{\gamma}_{ll,i}}{1 + 2\bar{\gamma}_{ll,i}} + 1} \right) \qquad (28)$$

where $V_{ll,i} = [2, 1, -1, -1, 1]$ is index vector.

B. OUTAGE PROBABILITY BASED ON SUM RATE ANALYSIS

In this sub-section, the outage probability is a criterion for the evaluation of the quality of service [55]. It measures the probability of losing out to arrive at an output SNR threshold value required for a desired service.

$$Pr_{out} = p_r(\gamma_{SNR} \leq \gamma_{min}) \qquad (29)$$

where the γ_{min} is a threshold SNR criterion, for received SNR below γ_{min}, the received symbols cannot be successfully decoded with probability one, and the system declares an outage. We define the outage probability in equation (29), i,e. The probability that the rate of at least one BSP is lower than its minimum required rate. For the SNR above γ_{min}, the received symbols can be successfully decoded with probability one [56]. For a single user, the channel capacity for BSP that normalized the capacity using Shannon's law is given as below

$$C_{PTP} = B \log_2 \left(1 + \frac{P_T G^2}{N_0} \right) \qquad (30)$$

where C_{PTP} is the point-to-point channel capacity in bits per second per Hz (bps/Hz), B is the channel bandwidth in Hz and G is the channel gain, and P_T is the transmitted total power. Also, it is assumed that noise is additive Gaussian with a variance N_0. For two users, taking into account the interference caused by another user, and modeling it Gaussian, its power will appear and it is added to N_0 in the denominator. Each BSP in a multiple access channel can transmit at a rate ($C \leq R$) inequality [57]. A point-to-multi-point (PTM) channel distribution BSP is composed of one transmit point and ($j > 1$) receive points. In such a network, collaboration among the received points may improve the power gain and thus the capacity gain. Denote G_j as the channel coefficient of receive point j with unit variance, and all the $G_j(j = 1, 2, 3..J)$ follow the same distribution. Total capacity framework for a PTM based on Shannon's law is written as below

$$C_{PTM} = \frac{B}{N} \log_2 \left(1 + \sum_{j=1}^{J} \frac{P_T G_j^2}{N_0} \right) \qquad (31)$$

The total capacity now can be described as $C \sim N(\overline{C}, \sigma_c^2)$, mean $\overline{C}$ and σ_c^2 noise variance. Hence, outage probability based on capacity [58], it can be defined as following

$$Pr_{out} = p_r(C < \gamma_R) = 1 - Q \left(\frac{\gamma - \overline{C}}{\sigma_c} \right) \qquad (32)$$

$$\overline{C} = \frac{1}{N} \sum_{i=1}^{M} C_i \qquad (33)$$

where in γ_R is the threshold rate value, and $Q(\cdot)$ is the standard Q function. C_i denotes the total capacity as the summation of M RBs capacities. Finally, $\overline{C}$ is the average total capacity. For diverse BSPs transmitting simultaneously, a multiple access rate region is characterized by all the upper bounds on the rates based on the Shannon's rate law. Since there are LDM and FeMBMS layers in the hybrid system, the total sum rate is a summation of the RBs rate for each layer as below

$$R_T = R_{LDM} + R_{FeMBMS} \qquad (34)$$

where R_{LDM} and R_{FeMBMS} denotes the sum rate of LDM and FeMBMS parts, respectively. We assume ($\overline{C}_{PTM} \leq R_T$) is inequality threshold rate value, which R_T is concerning to γ_R. outage probability as the average of instantaneous PTM capacities that is less than the threshold rate value as below

$$Pr_{out} = p_r(\overline{C}_{PTM} < R_0) \qquad (35)$$

The sum rate of the FeMBMS part, based on Shannon's rate formula, can be written as below

$$R_{FeMBMS} = \frac{B}{N} \sum_{n=1}^{N_{FeMBMS}} R_{FeMBMS}[n] \qquad (36)$$

inequality for outage probability that satisfies this condition is given by

$$R_{FeMBMS}[n] < R_0 \qquad (37)$$

Therefore, the outage probability of the total number of FeM-BMS sub-carriers for each RBs can be expressed as

$$Pr_{out}^{FeMBMS} = \frac{1}{N_{FeMBMS}} \sum_{n=1}^{N_{Fe.}} Pr\{R_{FeMBMS}[n] < R_0\} \quad (38)$$

where

$$\gamma_{FeMBMS}[n] = \frac{p_{FeMBMS} G_{FeMBMS}[n]}{N_0^{ps}} \quad (39)$$

is the SNR per sub-carrier for FeMBMS received power and received noise. Also, $p_{FeMBMS} = P_T \frac{\Omega}{M} \frac{1}{N_{FeMBMS}}$, for all $k \in \{1, 2, \ldots, N_{FeMBMS}\}$ denotes the transmit power per FeMBMS sub-carrier, $N_{FeMBMS} = \Omega N_m$ denotes the total number of FeMBMS sub-carriers, and $N_0^{ps} = N_0 \frac{1}{N}$ denotes the noise power per sub-carrier. The sum rate of the LDM part can be written as

$$R_{LDM} = \frac{B}{N} \sum_{k=1}^{N_{LDM}} \left[\log_2(1 + \gamma_{LL}[n]) \right.$$
$$\left. + \log_2(1 + \gamma_{UL}[n]) \right] \quad (40)$$

$$\gamma_{LL}[n] = \frac{p_{LL} G_{LL}[n]}{N_0^{ps}} \quad (41)$$

where $\gamma_{LL}[n]$ is the SNR per subcarrier for LL of LDM received power $p_{LL} E\{|H_{LL}[n]|^2\}$ or power density spectrum multiply input signal and received noise N_0^{ps} and $\gamma_{UL}[n]$ is the SINR per subcarrier of UL of LDM received power and LL interference plus received noise is given by

$$\gamma_{UL}[n] = \frac{p_{UL} G_{UL}[n]}{p_{LL} G_{UL}[n] + N_0^{ps}} \quad (42)$$

Moreover, $p_{LL} = P_{LL} \frac{1}{N_{LDM}}$ and $p_{UL} = P_{UL} \frac{1}{N_{LDM}}$, for all $k \in \{1, 2, \ldots, N_{LDM}\}$ denotes the transmit powers per sub-carrier of LL and UL, and $N_{LDM} = \Psi N_m$ denotes the total number of LDM sub-carriers. Moreover in second part $P_{UL} E\{|H_{UL}[n]|^2\}$ is receiving power and N_0^{ps} is receiving noise power from UL, $P_{LL} E\{|H_{UL}[n]|^2\}$ as a interfere noise to UL from LL for decoding in SIC receiver.

$$R_{LDM}[n] = log_2 \left(1 + \frac{p_{LL} G_{LL}[n]}{N_0^{ps}} \right)$$
$$+ log_2 \left(1 + \frac{p_{UL} G_{UL}[n]}{p_{LL} G_{UL}[n] + N_0^{ps}} \right)$$
$$n = 1, 2, 3, \ldots, N_{LDM} \quad (43)$$

where $G_{LL}[n] = E\{|H_{LL}[n]|^2\}$ and $G_{UL}[n] = E\{|H_{UL}[n]|^2\}$. The outage probability for the total number of LDM subcarriers can be defined as below

$$Pr_{out}^{LDM} = \frac{1}{N_{LDMS}} \sum_{n=1}^{N_{LDM}} Pr\{R_{LDM}[n] < R_0\} \quad (44)$$

For the overall proposed system, outage probability can be expressed as below

$$Pr_{out}^{overall} = \frac{1}{N} \left[\sum_{n=1}^{N_{FeMBMS}} Pr\{R_{FeMBMS}[n] < R_0\} \right.$$
$$\left. + \sum_{n=1}^{N_{LDM}} Pr\{R_{LDM}[n] < R_0\} \right] \quad (45)$$

Which $\forall n \epsilon \{1, 2, 3, \ldots K\}$ is a number of sub-carriers and R_0 is a minimum threshold required data for outage performance.

C. COVERAGE PROBABILITY

Coverage probability is defined as the probability of typical mobile UDs reaching the SINR threshold. We change this definition a bit and say that a typical user might reach the target rate of the threshold R_0 [59]. The coverage probability is done as a supplement to outage probability with a simple calculation as following

$$P_{cov}^{LDM} = 1 - Pr_{out}^{LDM} \quad (46)$$
$$P_{cov}^{FeMBMS} = 1 - Pr_{out}^{FeMBMS} \quad (47)$$
$$P_{cov}^{overall} = 1 - Pr_{out}^{overall} \quad (48)$$

V. FTPA LDM POWER ALLOCATION ALGORITHM

As shown in Figures 9 and 10, the effect of FTPA over LDM BER performance is assessed. FTPA is a fast algorithm for power allocation in LDM downlink. Due to its low computational complexity, it is widely adopted in multiple radio access systems. By applying the FTPA algorithm [54], the transmit power of LDM, RBs on sub-carrier kth (SC_k) is assigned pursuant to the channel profits are $\{|H_{LL}|^2, |H_{UL}|^2\}$ of all the multiplexed users on SCk, which is given as

$$P_{UL} = P_{LDM} \frac{E\{|H_{UL}|^2\}^{-\xi}}{E\{|H_{UL}|^2\}^{-\xi} + E\{|H_{LL}|^2\}^{-\xi}} \quad (49)$$

$$P_{LL} = P_{LDM} - P_{UL} \quad (50)$$

where $\xi \ (0 \le \xi \le 1)$ is a decline factor and in the case of $\xi = 0$, it is put through identical power. Here we select it as $\xi = 0.4$. As can be seen from equation (49) the FTPA method is based on the rule that when ξ increases. Generally, more power is allocated to the user with poorer CRNN and also low power is assigned to the stronger CRNN coefficients, which can be written according to the average SNR definition in equations (14)–(18). By using the FTPA method, we provide two different services i.e. fixed and variable modes. When the fixed mode is used, we allocate power to LL,UL layers with a constant coefficient as = 0.4 and = 0.6 respectively. When the variable mode is used, we change the UL from 0 to -3, -5, and -7 dB respectively while the LL keeps at 0 dB. For the sake of the UL changes, various mobile broadcast services can be provided from SDTV to UHDTV [54].

TABLE 3. Simulation Parameters.

Parameter	Value
System Bandwidth	5 MHz
Transmitter P_{Tmax}	46 dBm
Number of total Resource blocks: M	16
FFT size : N	8192
Center frequency f_0	2.1GHz
Total number of users U for equal LDM/FeMBMS allocation	24
E_b/N_0	$0-24$ dB
Modulation LDM two layers and FeMBMS	QPSK/BPSK/QPSK
ACCP =Attenuation Path Loss(APL)	$E\left\{|H_{LL}|^2\right\} = 0$ dB
$(ACCP)_{UL}=$ Attenuation Path Loss (APL)	$E\left\{|H_{UL}|^2\right\} = 0, -3, -5, -7$ dB
$(ACCP)_{FeMBMS}=$ Attenuation Path Loss (APL)	$E\left\{|H_{FeMBMS}|^2\right\} = 0$ dB
Sub carriers separation $\triangle f$	$0.97\,KHz$
Channel model/fading	Rayleigh small scale frequency selective fading
Recipient	General Multi-carrier + SIC
Gain amplitude (g) for LDM	between 0 and 1
Number of sub carriers per RBs: K_m	512

VI. SIMULATION RESULTS

Simulation parameters are listed in Table 3. In our scenario, we concentrate on cellular broadcast hybrid technology. We assign half of the sub-carriers to FeMBMS and the others to LDM with equal power allocation for all sub-carriers. The gNB is located in a single cell with a SISO antenna structure. We simulated downlink FeMBMS/LDM over a multipath Rayleigh fading channel [60]. The channel fading gains are modeled as small-scale multipath frequency selective fading. Two BSPs seek to provide service to their subscribed users. Users are uniformly distributed in a hexagonal cellular area with a unit length. The simulation based on MATLAB software shows that the exact closed-form BER and outage performance expressions are matched to the theoretical completely. To present the benefits of hybrid multiple-access technology selections, the achieved utility of the proposed framework is compared to the LDM and FeMBMS cases. All statistical results are averaged over a large number of independent runs. To illustrate the performance gains, we use simulation results for various LDM/FeMBMS hybrid setups. The BER and achievable sum rate are considered for this purpose. The results of primary performance metrics will be coming in the following three sub-sections: in subsection A, BER performance, in sub-section B, FTPA method for LDM multi-services, and in sub-section C, Outage and coverage performance are brought up.

A. BER PERFORMANCE

As illustrated in Figure 4, the BER proficiency of BPSK-BPSK/QPSK modulation orders three services for two layers LDM and FeMBMS are compared with the hybrid proposed framework against the $Eb/N0$ (dB). When $Eb/N0$ (dB) is
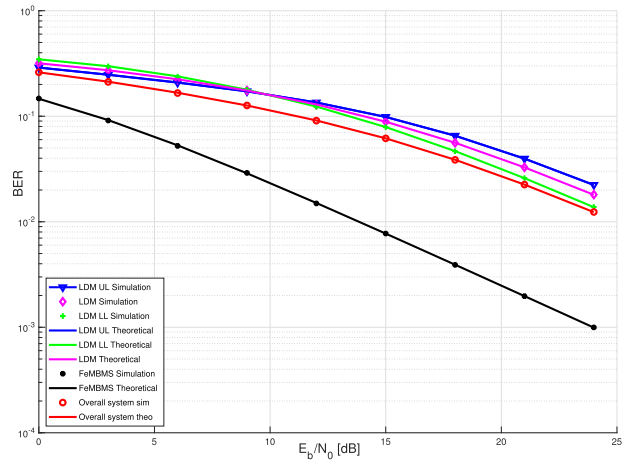

FIGURE 4. BER proficiency LDM/FeMBMS hybrid layers for BPSK-BPSK Modulation versus E_b/N_0.

increased, the FeMBMS BER proficiency improves compare to the LDM and the proposed hybrid framework remarkably.

Figure 5, shows the BER performance of QPSK-BPSK/QPSK modulation schemes for LDM and FeMBMS are considered with the hybrid proposed framework against the $Eb/N0$ (dB). When $Eb/N0$ (dB) is increased, the FeMBMS BER performance improves then the LDM and the proposed hybrid framework considerably. It is obvious that the simulation, and theory for LDM-LL,LDM-UL,FeMBMS services, and the overall system are matched exactly.

Figure 6, depicts, the BER performance of QPSK-QPSK/QPSK modulation schemes for LDM and FeMBMS are considered with the hybrid proposed framework versus the $Eb/N0$ (dB). When $Eb/N0$ (dB) increases, FeMBMS BER performance reclaims then the LDM and the proposed hybrid framework substantially, which shows a miss-match problem in LDM-LL, in simulation and theory. But for LDM-UL and FeMBMS layers and overall system are matched exactly. Figure 7, demonstrates the BER performance of the LDM layers versus $Eb/N0$ (dB) under different numbers of receiving antennas at the BS. In our scenario, we assume the number of RBs for LDM and FeMBMS are equal to $\Omega = \Psi = 8$. block/s. Also, shows that, both theoretical and simulation LDM-UL and LDM-LL and LDM results are matched completely. In each sub-carrier, LDM technology has the potential to support two users. Hence, there is facilitating meeting sum rate for requirements of two mobile and fixed services. Since we use QPSK and BPSK modulations for near user and UL (far user), the bits per symbol for both layers are denoted as $k_{LL} = \log_2 4 = 2$ and $k_{UL} = \log_2 2 = 1$, respectively.

Although we use SIC for LDM users, residual interference causes BER performance degradation, therefore from Figure 8, As can be seen, for the proposed method, there is a curve between both technologies, and the efficiency is better than LDM, and FeMBMS.
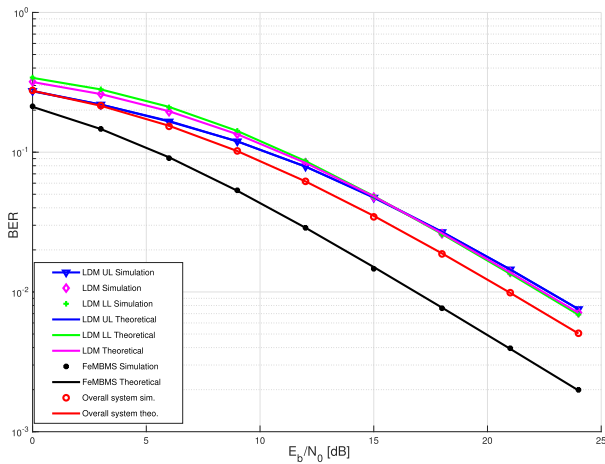
FIGURE 5. BER proficiency LDM/FeMBMS hybrid layers for QPSK-BPSK Modulation versus E_b/N_0.
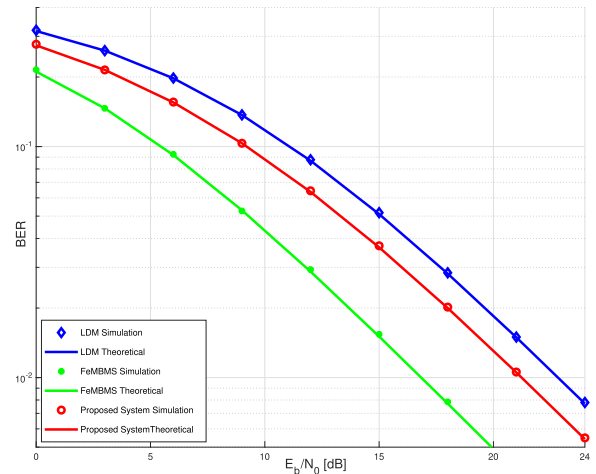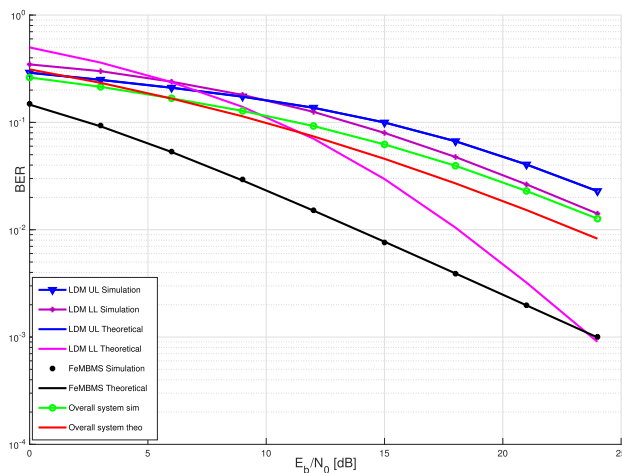

FIGURE 6. BER proficiency LDM/FeMBMS hybrid layers for QPSK-QPSK Modulation versus E_b/N_0.
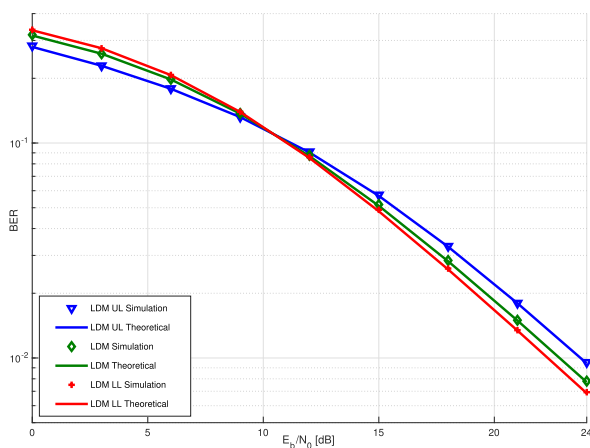

FIGURE 7. BER proficiency of LDM layers versus E_b/N_0.

B. FTPA ALGORITHM RESULTS FOR LDM
Figures 9 and 10 analyzes the effect of the FTPA and without FTPA on BER performance to obtain P_{LL} and P_{UL} power

FIGURE 8. BER proficiency of offering service compared with LDM/FeMBMS separately versus E_b/N_0.

allocation for LDM layers. Figure 9 indicates the impact of FTPA on BER performance for the UL layer with different path losses. In this study, we assumed LL to be set 0 dB, while UL changes are $(-3, -5, -7)$ dB, which are called attenuation path loss $E\left\{|H_{UL}|^2\right\} = -3, -5, -7$dB, or ACCP gain. Moreover Figure 9, shows that BER performance with FTPA in the UL equals to -3 dB path loss. The FTPA affects BER performance UL but has no effect on LL. Hence, results reveal that the -3dB value outperformed -5,-7 dB in terms of BER performance. As shown in Table 3 is brought, power allocation PLL and PUL values were evaluated by the FTPA and diverse path losses are given $E\left\{|H_{UL}|^2\right\} = -3, -5, -7$ dB. Furthermore, fixed power allocation values, without FTPA given as $P_{LL} = 0.4$ and $P_{UL} = 0.6$. As shown in Figure 10, the results regarding the effect of the FTPA method on BER performance for LDM layers with different path losses are obtained. In this scenario, we consider LL to be set 0 dB, while LDM changes are $(-3, -5, -7)$ dB, attenuation path loss, or ACCP gain. As shown in Figure 10, in these scheme the BER performance of the LDM part with different attenuation levels is evaluated for the UL channel with/without the FTPA method. It is assumed that the user in the UL channel is located far from the BS; therefore, path loss attenuation is found to will be high. When the UL is searching for different path losses $(-3, -5, -7)$ dB, the user in LL is set to 0 dB. As illustrated in Figure 10, the lowest performance and best path loss for the LDM are $-7, -3$ dB, respectively. The closed-form equation for simulation and theory outperforms the BER performance of the LDM, in comparison with the UL channel.

Figure 11 depicts the results of the overall system as well as various numbers of FeMBMS RBs allocations. In this simulation, the number of engaged RBs is $M = 16$ for every scenario, but the number of FeMBMS RBs, Ω, is continuously derived {0, 4, 8, 12, 16}. Thus, the number of LDM RBs, Ψ, is obtained as {16, 12, 8, 4, 0}. It is evident that when the number of FeMBMS RBs, Ω increases,
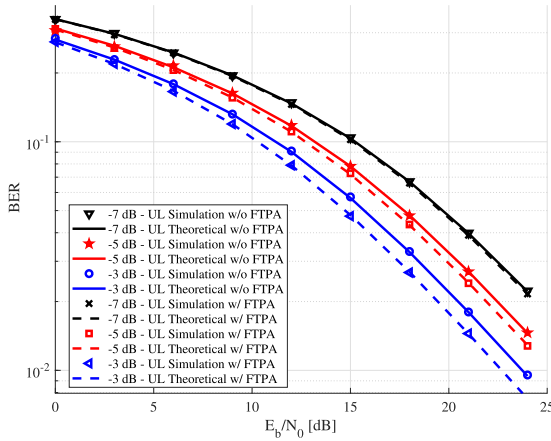
FIGURE 9. BER performance of UL part with different channel gain for UL with/without FTPA versus E_b/N_0.
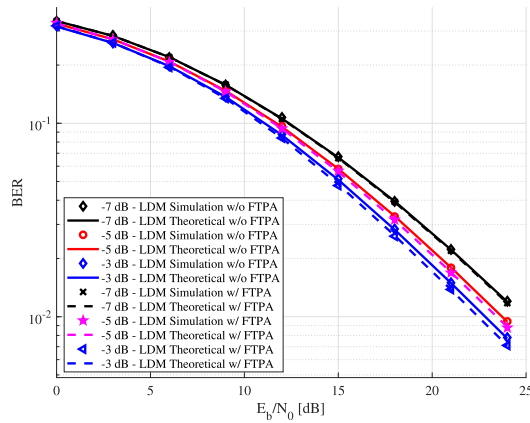

FIGURE 10. BER performance of LDM of proposed system with different channel gain for UL channel with/ without FTPA versus E_b/N_0.

TABLE 4. Impact of Fix Power Allocation.

Parameter	Value		
ACCP of $E\left\{|H_{UL}|^2\right\}$[dB]=Path Loss	-3	-5	-7
P_{LL}	0.4	0.4	0.4
P_{UL}	0.6	0.6	0.6
ACCP of $E\left\{|H_{LL}|^2\right\}$[dB]=Path Loss	0dB		

TABLE 5. Impact of FTPA method.

Parameter	Value		
ACCP of $E\left\{|H_{UL}|^2\right\}$[dB]=Path Loss	-3	-5	-7
P_{LL}	0.3625	0.3801	0.3961
P_{UL}	0.6375	0.6199	0.6039
ACCP of $E\left\{|H_{LL}|^2\right\}$[dB]=Path Loss	0dB		

the proposed hybrid system improves BER performance. However, a decrease in the number of LDM RBs, Ψ, outperforms the BER performance of the proposed hybrid framework.
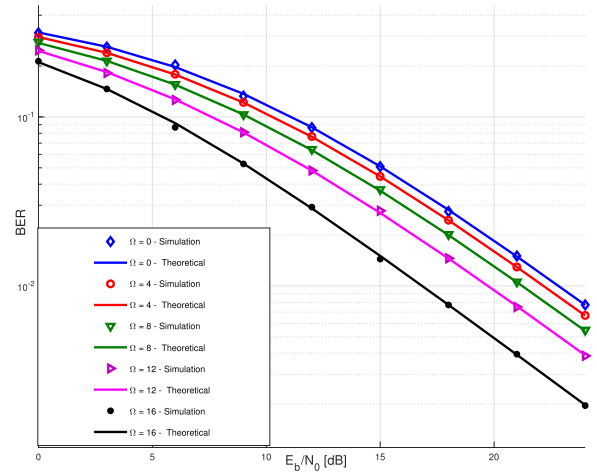
FIGURE 11. BER proficiency of offering service against E_b/N_0 with different number of FeMBMS RBs.
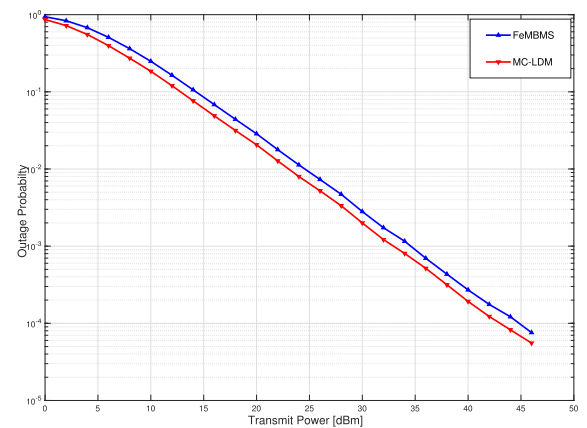

FIGURE 12. Outage probability for LDM /FeMBMS versus $P_T max$.
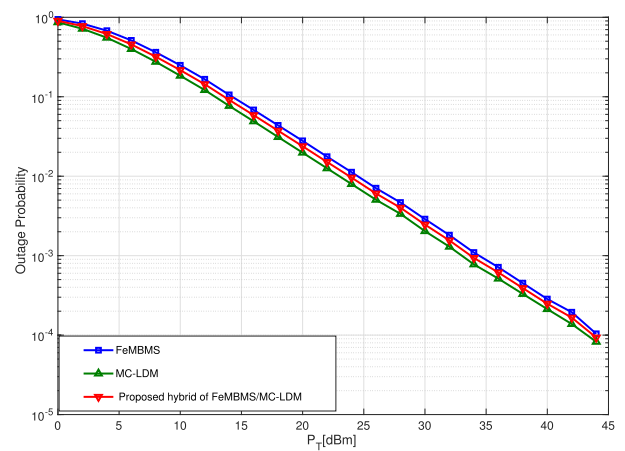

FIGURE 13. Outage probability for LDM/ FeMBMS as individually and hybrid proposed system versus $P_T max$.

C. OUTAGE AND COVERAGE PROBABILITY

Figure 12 indicates that the outage probability against the maximum transferred power. It is illustrated that LDM is
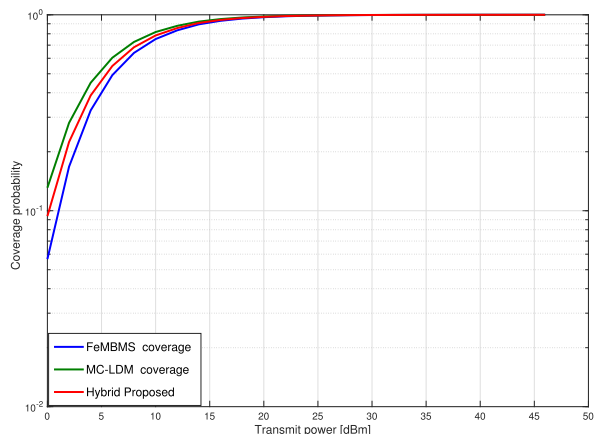
FIGURE 14. Coverage probability for LDM/eMBMS as individually and hybrid proposed system versus $P_T max$.
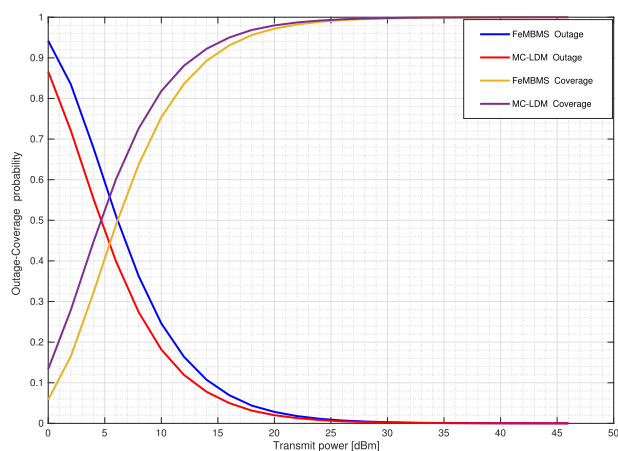

FIGURE 15. Outage-coverage probability for LDM/ FeMBMS as individually versus $P_T max$.

more efficient than the FeMBMS. It can be observed that the FeMBMS and LDM simultaneously carry one user and two users per sub-carrier, respectively. Hence, the two layers LDM were accompanied by an increment in their efficiencies in comparison with the FeMBMS single-layer mobile system. Therefore, it is concluded that the performance of LDM outage probability is better than that of the FeMBMS outage probability system. Figure 13 compares outage probability LDM and FeMBMS and hybrid both versus the maximum transmitted power. Also figure 13 shows that the proposed scheme provides the median outage probability owing to the flexibility in the RAT selection. The LDM outage outperforms while the FeMBMS outage has increased since FeMBMS and LDM concurrently carry one user and two users on the sub-carrier, respectively. Outage efficiency suggested combination service was demonstrated over the multi-path Rayleigh channel for multi-service, improving outage intermediate framework improves performance compared with the LDM and FeMBMS, individually. Figure 14 illustrates coverage probability for the hybrid proposed system, which shows LDM coverage performance is increased

compared to the other FeMBMS and the hybrid proposed system. As shown in Figure 15 compares the outage/coverage probability for LDM and FeMBMS versus total transmitted power, which is LDM and FeMBMS coverage are inversely with outage probability. It can be derived that LDM coverage performance is better than the FeMBMS also the FeMBMS outage probability has better performance than the LDM technology.

VII. CONCLUSION

In this analysis, we introduced a hybrid approach for 5G broadcasting that has the ability to select services for two different user groups. This technology works based on average channel conditions. In the form of typical multiplexing, we considered and tested two technologies LDM-NOMA and FeMBMS-OMA. Unlike some of the works found in the literature, this paper emphasizes a compatible alternative middle structure layer without hardware complexity and cost less. We examined the effect of two BSP using single-cell broadcasting on the Rayleigh fading channel with the multi-path system. Mathematical analysis, based on the exact closed-form expressions, is consistent with the theory of the proposed framework. The simulation results are based on the Monte Carlo iterative methodology and demonstrated the superiority of the hybrid framework compared to the LDM-NOMA and FeMBMS-OMA individual schemes. It can be concluded that the performance of hybrid orthogonal/non-orthogonal framework technology is better than a sole technology in terms of BER and sum rate and outage/coverage probability based on stochastic geometry. Therefore, it is recommended that this technology be incorporated into the next-generation cellular 5G broadcast. Future work can extend to the case of more than two users sharing one sub-carrier per RB in LDM/FeMBMS.

REFERENCES

[1] (Nov. 2022). *Ericsson Mobility Report-Leading Telecom Industry Data*. [Online]. Available: http://www.ericsson.com

[2] (2021). *ROHDE & SCHWARZ 5G Broadcast/Multicast*. [Online]. Available: http://www.Rohde-schwarz.com/support

[3] (May 2021). *QCOMReseach Pioneering 5G Broadcast*. [Online]. Available: https://www.qualcomm.com/blog

[4] A. Roy, P. Chaporkar, and A. Karandikar, "Optimal radio access technology selection algorithm for LTE-WiFi network," *IEEE Trans. Veh. Technol.*, vol. 67, no. 7, pp. 6446–6460, Jul. 2018.

[5] U. Meabe, X. Gil, C. Li, M. Vélez, and P. Angueira, "On the coverage and cost of HPHT versus LPLT networks for rooftop, portable, and mobile broadcast services delivery," *IEEE Trans. Broadcast.*, vol. 61, no. 2, pp. 133–141, Jun. 2015. [Online]. Available: http://ieeexplore.ieee.org/document/7047756/

[6] S. Parkvall, E. Dahlman, A. Furuskar, and M. Frenne, "NR: The new 5G radio access technology," *IEEE Commun. Standards Mag.*, vol. 1, no. 4, pp. 24–30, Dec. 2017.

[7] L. Shi, E. Obregon, K. W. Sung, J. Zander, and J. Bostrom, "CellTV—On the benefit of TV distribution over cellular networks: A case study," *IEEE Trans. Broadcast.*, vol. 60, no. 1, pp. 73–84, Mar. 2014, doi: 10.1109/TBC.2013.2295255.

[8] M. H. Alsharif and R. Nordin, "Evolution towards fifth generation (5G) wireless networks: Current trends and challenges in the deployment of millimetre wave, massive MIMO, and small cells," *Telecommun. Syst.*, vol. 64, no. 4, pp. 617–637, Apr. 2017.

[9] International Telecommunication Union. (2012). *Digital Dividend: Insights for Spectrum Decisions*. [Online]. Available: http://www.itu.int/ITU-D/tech/digital_broadcasting/DigitalDividend.pdf

[10] H. Shariatzadeh, S. Ghazi-Maghrebi, and B. Karakaya, "An improving performance cellular DTV broadcasting with hybrid non-orthogonal LDM and orthogonal eMBMS configuration," *Array*, vol. 11, Sep. 2021, Art. no. 100073, doi: 10.1016/j.array.2021.100073.

[11] A. Domínguez, J. Flórez, A. Lafuente, S. Masneri, I. Tamayo, and M. Zorrilla, "A methodology for user interface adaptation of multi-device broadcast-broadband services," *IEEE Access*, vol. 8, pp. 211048–211062, 2020, doi: 10.1109/ACCESS.2020.3039616.

[12] (2016). *Handbook on Digital Terrestrial Television Broadcasting Networks and Systems Implementation*. [Online]. Available: https://www.itu.int/dms_pub/itu-r/oth/R0A0700003B0001PDFE.PDF

[13] M. El-Hajjar and L. Hanzo, "A survey of digital television broadcast transmission techniques," *IEEE Commun. Surveys Tuts.*, vol. 15, no. 4, pp. 1924–1949, 4th Quart., 2013. [Online]. Available: http://ieeexplore.ieee.org/document/6492307/

[14] *Architectural Enhancements for 5G Multicast-Broadcast Services*, 3GPP, document ETSI TS 123 247, 2022.

[15] D. Gomez-Barquero, J. Lee, S. Ahn, C. Akamine, D. He, J. Montalaban, J. Wang, W. Li, and Y. Wu, "IEEE transactions on broadcasting special issue on: Convergence of broadcast and broadband in the 5G era," *IEEE Trans. Broadcast.*, vol. 66, no. 2, pp. 383–389, Jun. 2020, doi: 10.1109/TBC.2020.2985493.

[16] X. Wei, H. Al-Obiedollah, K. Cumanan, M. Zhang, J. Tang, W. Wang, and O. A. Dobre, "Resource allocation technique for hybrid TDMA-NOMA system with opportunistic time assignment," in *Proc. IEEE Int. Conf. Commun. Workshops (ICC Workshops)*, Jun. 2020, pp. 1–6.

[17] L. Zhang, W. Li, Y. Wu, Y. Xue, E. Sousa, S.-I. Park, J.-Y. Lee, N. Hur, and H.-M. Kim, "Using non-orthogonal multiplexing in 5G-MBMS to achieve broadband-broadcast convergence with high spectral efficiency," *IEEE Trans. Broadcast.*, vol. 66, no. 2, pp. 490–502, Jun. 2020, doi: 10.1109/TBC.2020.2983563.

[18] M. Zeng, A. Yadav, O. A. Dobre, and H. V. Poor, "Energy-efficient joint user-RB association and power allocation for uplink hybrid NOMA-OMA," *IEEE Internet Things J.*, vol. 6, no. 3, pp. 5119–5131, Jun. 2019, doi: 10.1109/JIOT.2019.2896946.

[19] S. Pandya, M. A. Wakchaure, R. Shankar, and J. R. Annam, "Analysis of NOMA-OFDM 5G wireless system using deep neural network," *J. Defense Model. Simul., Appl., Methodol., Technol.*, vol. 19, no. 4, pp. 799–806, Oct. 2022.

[20] D. Gomez-Barquero, D. Navratil, S. Appleby, and M. Stagg, "Point-to-multipoint communication enablers for the fifth generation of wireless systems," *IEEE Commun. Standards Mag.*, vol. 2, no. 1, pp. 53–59, Mar. 2018.

[21] *5G; NR; Services Provided by the Physical Layer*, 3GPP, document TS 138 202, 2020.

[22] J. Calabuig, J. F. Monserrat, and D. Gómez-Barquero, "5th generation mobile networks: A new opportunity for the convergence of mobile broadband and broadcast services," *IEEE Commun. Mag.*, vol. 53, no. 2, pp. 198–205, Feb. 2015.

[23] J. C. Gaspar, "Broadcasting in 4G mobile broadband networks and its evolution towards 5G," Ph.D. dissertation, Departamento de Comunicaciones, Universitat Politècnica de València, Valencia, Spain, Mar. 2015. [Online]. Available: https://riunet.upv.es/handle/10251/48561

[24] J. J. Gimenez, J. L. Carcel, M. Fuentes, E. Garro, S. Elliott, D. Vargas, C. Menzel, and D. Gomez-Barquero, "5G new radio for terrestrial broadcast: A forward-looking approach for NR-MBMS," *IEEE Trans. Broadcast.*, vol. 65, no. 2, pp. 356–368, Jun. 2019. [Online]. Available: https://ieeexplore.ieee.org/document/8705278/

[25] L. Zhang, Y. Wu, G. K. Walker, W. Li, K. Salehian, and A. Florea, "Improving LTE eMBMS with extended OFDM parameters and layered-division-multiplexing," *IEEE Trans. Broadcast.*, vol. 63, no. 1, pp. 32–47, Mar. 2017. [Online]. Available: http://ieeexplore.ieee.org/document/7792158/

[26] L. Zhang, W. Li, Y. Wu, K. Salehian, S. Laflèche, Z. Hong, S. Park, H. M. Kim, J. Lee, N. Hur, X. Wang, P. Angueira, and J. Montalban, "Using layered-division-multiplexing to deliver multi-layer mobile services in ATSC 3.0," *IEEE Trans. Broadcast.*, vol. 65, no. 1, pp. 40–52, Mar. 2019. [Online]. Available: https://ieeexplore.ieee.org/document/8423697/

[27] E. C. Cejudo, H. Zhu, J. Wang, and O. Alluhaibi, "A fast algorithm for resource allocation in downlink multicarrier NOMA," in *Proc. IEEE Wireless Commun. Netw. Conf. (WCNC)*, Apr. 2019, pp. 1–5.

[28] Z. Shen, J. G. Andrews, and B. L. Evans, "Adaptive resource allocation in multiuser OFDM systems with proportional rate constraints," *IEEE Trans. Wireless Commun.*, vol. 4, no. 6, pp. 2726–2737, Nov. 2005, doi: 10.1109/TWC.2005.858010.

[29] M. Baghani, S. Parsaeefard, M. Derakhshani, and W. Saad, "Dynamic non-orthogonal multiple access and orthogonal multiple access in 5G wireless networks," *IEEE Trans. Commun.*, vol. 67, no. 9, pp. 6360–6373, Sep. 2019, doi: 10.1109/TCOMM.2019.2919547.

[30] S. H. Kim and J. Kim, "An opportunistic MCS drop scheme for improved LTE eMBMS transmission," *Wireless Pers. Commun.*, vol. 107, no. 3, pp. 1431–1442, Aug. 2019, doi: 10.1007/s11277-018-5973-1.

[31] J. Ghosh, V. Sharma, H. Haci, S. Singh, and I. Ra, "Performance investigation of NOMA versus OMA techniques for mmWave massive MIMO communications," *IEEE Access*, vol. 9, pp. 125300–125308, 2021, doi: 10.1109/ACCESS.2021.3102301.

[32] F. Kara and H. Kaya, "BER performances of downlink and uplink NOMA in the presence of SIC errors over fading channels," *IET Commun.*, vol. 12, no. 15, pp. 1834–1844, Sep. 2018.

[33] M. Jain, S. Soni, N. Sharma, and D. Rawal, "Performance analysis at far and near user in NOMA based system in presence of SIC error," *AEU-Int. J. Electron. Commun.*, vol. 114, Feb. 2020, Art. no. 152993, doi: 10.1016/j.aeue.2019.152993.

[34] X. Guo and Y. Luo, "Hybrid NOMA/OFDMA visible light communication system with coordinated multiple point transmission," *Opt. Exp.*, vol. 30, pp. 47404–47420, Jan. 2022.

[35] C. Chen, "Fairness-aware hybrid NOMA/OFDMA for bandlimited multi-user VLC systems," *Opt. Exp.*, vol. 29, pp. 42265–42275, May 2021.

[36] H. T. H. Giang, T. N. K. Hoan, P. D. Thanh, and I. Koo, "Hybrid NOMA/OMA-based dynamic power allocation scheme using deep reinforcement learning in 5G networks, *Appl. Sci.*, vol. 10, vol. 7, p. 4236, 2020, doi: 10.3390/app10124236.

[37] A. Tusha, S. Dogan, and H. Arslan, "A hybrid downlink NOMA with OFDM and OFDM-IM for beyond 5G wireless networks," *IEEE Signal Process. Lett.*, vol. 27, pp. 491–495, 2020, doi: 10.1109/LSP.2020.2979059.

[38] A. Shokair, M. Crussière, J. Hélard, Y. Nasser, and O. Bazzi, "Analysis of hybrid broadcast/broadband networks with multiple broadcasting stations," *IEEE Access*, vol. 7, pp. 141226–141240, 2019.

[39] Z. Q. Al-Abbasi and D. K. C. So, "Resource allocation in non-orthogonal and hybrid multiple access system with proportional rate constraint," *IEEE Trans. Wireless Commun.*, vol. 16, no. 10, pp. 6309–6320, Oct. 2017. [Online]. Available: http://ieeexplore.ieee.org/document/7968335/

[40] L. Bariah, S. Muhaidat, and A. Al-Dweik, "Error probability analysis of non-orthogonal multiple access over Nakagami-m fading channels," *IEEE Trans. Commun.*, vol. 67, no. 2, pp. 1586–1599, Feb. 2019, doi: 10.1109/TCOMM.2018.2876867.

[41] A. S. Marcano and H. L. Christiansen, "Impact of NOMA on network capacity dimensioning for 5G HetNets," *IEEE Access*, vol. 6, pp. 13587–13603, 2018, doi: 10.1109/ACCESS.2018.2799959.

[42] L. Zhang, W. Li, Y. Wu, Z. Hong, K. Salehian, X. Wang, P. Angueira, J. Montalban, M. Velez, S. Park, H. M. Kim, and J. Lee, "Performance characterization and optimization of mobile service delivery in LDM-based next generation DTV systems," *IEEE Trans. Broadcast.*, vol. 61, no. 4, pp. 557–570, Dec. 2015.

[43] *LTE; Multimedia Broadcast Multicast Services (MBMS) and Packet-Switched Streaming Service (PSS) Enhancements to Support Television Services*, 3GPP, document TR 126 917, 2018.

[44] Z. Zhang, Z. Ma, M. Xiao, G. Liu, and P. Fan, "Modeling and analysis of non-orthogonal MBMS transmission in heterogeneous networks," *IEEE J. Sel. Areas Commun.*, vol. 35, no. 10, pp. 2221–2237, Oct. 2017. [Online]. Available: http://ieeexplore.ieee.org/document/7971899/

[45] T. Assaf, A. J. Al-Dweik, M. S. E. Moursi, H. Zeineldin, and M. Al-Jarrah, "Exact bit error-rate analysis of two-user NOMA using QAM with arbitrary modulation orders," *IEEE Commun. Lett.*, vol. 24, no. 12, pp. 2705–2709, Dec. 2020.

[46] T. Maksymyuk, M. Brych, and V. Pelishok, "Stochastic geometry models for 5G heterogeneous mobile networks," *SmartCR*, vol. 5, pp. 89–101, Apr. 2015.

[47] J. Xu, J. Zhang, and J. G. Andrews, "On the accuracy of the Wyner model in cellular networks," *IEEE Trans. Wireless Commun.*, vol. 10, no. 9, pp. 3098–3109, Sep. 2011.

[48] Y. Hmamouche, M. Benjillali, S. Saoudi, H. Yanikomeroglu, and M. D. Renzo, "New trends in stochastic geometry for wireless networks: A tutorial and survey," *Proc. IEEE*, vol. 109, no. 7, pp. 1200–1252, Jul. 2021, doi: 10.1109/JPROC.2021.3061778.

[49] O. Somekh and S. Shamai (Shitz), "Shannon-theoretic approach to a Gaussian cellular multiple-access channel with fading," *IEEE Trans. Inf. Theory*, vol. 46, no. 4, pp. 1401–1425, Jul. 2000, doi: 10.1109/18.850679.

[50] D. Vargas and Y. J. D. Kim, "Two-layered superposition of broadcast/multicast and unicast signals in multiuser OFDMA systems," *IEEE Trans. Wireless Commun.*, vol. 19, no. 2, pp. 979–994, Feb. 2020. [Online]. Available: https://ieeexplore.ieee.org/document/8891918/

[51] F.-L. Luo and C. J. Zhang, *Signal Processing for 5G: Algorithms and Implementations*. Hoboken, NJ, USA: Wiley, 2016, pp. 143–157.

[52] B. Sklar, "Rayleigh fading channels in mobile digital communication systems. I. Characterization," *IEEE Commun. Mag.*, vol. 35, no. 7, pp. 90–100, Jul. 1997.

[53] D. Tse and P. Viswanath, *Fundamentals of Wireless Communication*. Cambridge, U.K.: Cambridge Univ. Press, May 2005, pp. 70–75.

[54] F. Fang, H. Zhang, J. Cheng, and V. C. M. Leung, "Energy-efficient resource allocation for downlink non-orthogonal multiple access network," *IEEE Trans. Commun.*, vol. 64, no. 9, pp. 3722–3732, Sep. 2016.

[55] S. Li, M. Derakhshani, S. Lambotharan, and L. Hanzo, "Outage probability analysis for the multi-carrier NOMA downlink relying on statistical CSI," *IEEE Trans. Commun.*, vol. 68, no. 6, pp. 3572–3587, Jun. 2020. [Online]. Available: https://ieeexplore.ieee.org/document/9031560/

[56] J. Wang, B. Xia, K. Xiao, Y. Gao, and S. Ma, "Outage performance analysis for wireless non-orthogonal multiple access systems," *IEEE Access*, vol. 6, pp. 3611–3618, 2018.

[57] M.-S. A. Marvin and K. Simon, *Digital Communication over Fading Channels*. Hoboken, NJ, USA: Wiley, 2005, pp. 18–20.

[58] H. Boostanimehr and V. K. Bhargava, "Outage capacity analysis for OFDM decode-and-forward systems in frequency selective Rayleigh fading channels," *IEEE Commun. Lett.*, vol. 16, no. 6, pp. 937–940, Jun. 2012.

[59] R. F. Guiazon, K.-K. Wong, and M. Fitch "Coverage probability of cellular networks using interference alignment under imperfect CSI," *Digital Commun. Netw.*, vol. 2, no. 4, pp. 162–166, 2016, doi: 10.1016/j.dcan.2016.10.007.

[60] Y. Yin, Y. Peng, M. Liu, J. Yang, and G. Gui, "Dynamic user grouping-based NOMA over Rayleigh fading channels," *IEEE Access*, vol. 7, pp. 110964–110971, 2019. [Online]. Available: https://ieeexplore.ieee.org/document/8793075/

SAEED GHAZI MAGHREBI was born in Iran, in 1963. He received the B.S. degree in electrical engineering from Kerman University, Iran, in 1988, the M.S. degree from the K. N. Toosi University of Technology, Iran, in 1995, and the Ph.D. degree in digital communications from Islamic Azad University, Iran, in 2010. He is currently the Dean of Islamic Azad University, Yadegar-e-Imam Khomeini (RAH) Share-Rey Branch, Tehran, Iran. He has published six books. His current research interests include digital communication, signal processing, and adaptive filtering. He has received the grade of the second degree of the 30th Khwarizmi International Award (KIA), in February 2017. He is the Designer of the Iranian National Data Centre.

HEYDAR SHARIATZADEH was born in Kermanshah, Iran, in 1964. He received the B.S. degree in electrical engineering from the Isfahan University of Technology, Iran, in 1995, and the M.Sc. degree in telecommunication and computer networks from the Iran University of Science and Technology, Tehran, Iran, in 2005. He is currently pursuing the Ph.D. degree in communication systems with Islamic Azad University, Tehran. From July 2019 to June 2020, he was a Visiting Researcher with the Department of Electrical and Electronics, Istanbul University-Cerrahpaşa. Since 1998, he has been a Lecturer with IRIB University and Islamic Azad University. He has also been a Technical Manager Engineer in planning of DTV networks in the Islamic Republic of Iran Broadcasting (IRIB) for a decade and pass training analog and DTV transmitters in Tokyo, Japan, from NEC Company, in 2009. He has published a book on DTTB. His current research interests include DTV cellular NOMA and 5G broadcast hybrid systems.

BAHATTIN KARAKAYA received the B.S., M.S., and Ph.D. degrees in electrical and electronic engineering from Istanbul University, Istanbul, Turkey, in 1998, 2002, and 2010, respectively. During his Ph.D. study, he collaborated with the WCSP Research Group, University of South Florida, Tampa, FL, USA. From 2011 to 2014, he was a Postdoctoral Researcher with Qatar University. Since May 2015, he has been an Assistant Professor with Istanbul University-Cerrahpaşa. His research interests include channel estimation, OFDM and SC-FDMA-based systems, cooperative communication, underwater acoustic communications, MIMO, and NOMA.

ALI SHAHZADI received the B.Sc., M.Sc., and Ph.D. degrees in electrical engineering from the Iran University of Science and Technology, in 1997, 2000, and 2005, respectively. He is currently an Associate Professor with Semnan University, Semnan, Iran. His main research interests include wireless, mobile and broadband communications and networking, digital signal processing, and artificial intelligence applications in communication theory.

• • •